A Hybrid Photovoltaic PV Array-Battery Powered EV-PMDC Drive Scheme

A. M. Sharaf, *Senior Member, IEEE,* E. Ozkop, and I. H. Altas, *Senior Member, IEEE*

***Abstract*--In this study, a hybrid photovoltaic PV array-battery powered PMDC drive scheme is realized. The PID tri loop limited current loop controller with motor current of four-wheel drive electric vehicle is used. Photovoltaic array and DC motor model are obtained in the Simulink. The proposed system control mechanism is digitally simulated by using the MATLAB/ Simulink/Sim-Power Systems software. The dynamic performance of the system is brought into at the constant speed reference and the variable speed reference trajectory.**

***Index Terms*— EV-PMDC, Photovoltaic, Drive control**

I. INTRODUCTION

THE demand for Electrical Energy and Fossil fuel has increased continuously during the last two or three decades with energy shortage, dwindling world fossil fuel and non-renewable natural resources. This has renewed interest in green Energy and Renewable/Alternative Wind, Photovoltaic, Fuel Cell, Bio-fuels and hybrid green energy schemes to supplement, complement and even replace fossil energy consumption in specific applications such as Transportation and Drive Systems. Extensive efforts in Energy Conservation, Demand Side Management and Efficient utilization, Loss Reduction can sustain the drive for LIVE-EARTH Renewal and Sustainability-Drive. Green House Gases, Water and Air Pollution and Rising Environmental Concerns are the motivating forces behind the Search for New Sustainable Energy. The traffic congestion problems have also grown and the increasing fuel cost did increase cost of living and acted as a Catalyst for New Technology Applications in Transportation Locomotive and Drive Sectors. The general view of the international oil industry regarding world oil reserves is even more alarming. The world oil market is expected to become a seller's market as early as 2006 and at the latest by 2016. Temporarily, the balance of power will shift towards Organization of Petroleum Exporting Countries (OPEC), but even the Middle East production is expected to start falling around 2010. A crisis in supply-demand balance is likely to emerge within 12 years as the impact of the growing demand of the developing economies competes with the high demand from developed countries for a dwindling supply [1].

In spite of the problems and concerns some of explained above, the majority of the world electricity is still generated by hydropower, fossil fuels and nuclear power in these times. Instead of using conventional energy sources, which are not renewable, environmentally friendly, theirs using cost are going rise, alternative energy resources such as wind, solar, geothermal, biomass and hydrogen energy should be used. The renewable energy sources share of total world energy consumption is expected to rise from 7 percent in 2004 to 8 percent in 2030 [2].

One of the example of alternative energy application is battery electric vehicles (BEVs) have zero vehicle emissions at the place of use. Lifecycle emissions depend on the electricity generation technology but reductions in both local and global pollutants can be achieved. Maintenance requirements are low and the reliability is high. Fuel costs are low. BEVs are quiet and with low vibrations. Electric vehicles can draw their energy from a variety of primary sources [1]. In this study, a Dual–DC-Photovoltaic array Source is used as drive electricity source. There are extensive studies relating to best EV-Electric Vehicle drive and locomotive systems [3-12].

DC motor is one of the machines convert the electrical energy to the mechanical energy. Nowadays, DC motor drive systems are widely used in many industry braches [13]. Years ago, most of the servo motors used for position control runs with alternative current (AC). Due to difficulties of control and nonlinear with AC motors, DC motors are preferred into some applications. But other side, because of the delicate mechanical Commutator & Brush Assembly of conventional DC motor requiring extensive maintenance and expensive repairs [14]. Thanks to development at DC motor technology and power electronics moment per volume of the motor has increased and permanent magnet motor types have been advanced, thus the Commutator & Brush Assembly maintenance/repair drawbacks have been largely reduced and in this way DC motor application area has further made wider. The DC motor speed or position control has been realized and also DC motor control methods have shown variety nowadays [15]. They include conventional PI, PID, fuzzy logic based, nonlinear, adaptive variable structure, model reference adaptive control, artificial neural networks, feed-forward torque/speed control strategies [16-21].

II. SYSTEM DESCRIPTION

The novel low cost independent PMDC four-wheel electric vehicle EV-PMDC drive system is shown in Fig. 1.

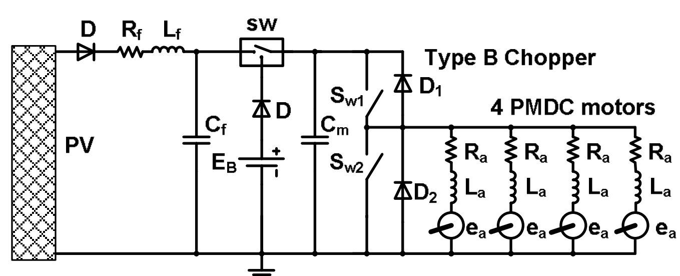

Fig. 1. The proposed four-wheel electric vehicle drive system.

The proposed system consists of four parts. There are DC voltage supply like a battery or photovoltaic (PV), DC-DC chopper, a controller and four PMDC motors for wheels. In this study, a photovoltaic array (PVA), type B-Dual Chopper and PMDC motor are used. PVA-Photovoltaic modules arranged in series and parallel to obtain the demand voltage and current ratings. A blocking diode (D) connected to PVA serially is used to block the reverse current flow. Input filter (R_f and L_f) allows for a valid quasi static model of the PVA and also acts as an added energy storage device. A capacitor (C_f) large value capacitor works an input filter and additional storage media [22]. There is a MOSFET of IGBT B type chopper with the controller. The output of controller is connected to loads four PMDC motors.

The schematic diagram of prototype four-wheel drive electric vehicle is shown in Fig. 2.

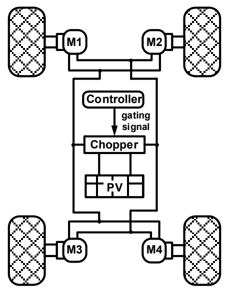

Fig. 2. Schematic diagram of prototype four-wheel drive electric vehicle.

A. DC Motor

DC motors have lots of desirable properties. Some of them are reliability, durable, inexpensive, and also using in low voltages, having positive conversion coefficients between electrical and mechanical, having size and design variation. For these reasons, the DC motors are utilized in many applications.

A permanent magnet dc motor (PMDC) is one of the DC motor types. PMDC system converts electrical power provided by a voltage source to mechanical power provided by a spinning rotor by means of magnetic coupling. The equivalent circuit of a PMDC motor is illustrated in Fig. 3. The parameters and symbols which were used in simulating the system are given in Appendix. The armature coil of the dc motor can be presented by an inductance (L_m) in series with resistance (R_a) in series with an induced voltage (e_m) which opposes the voltage source.

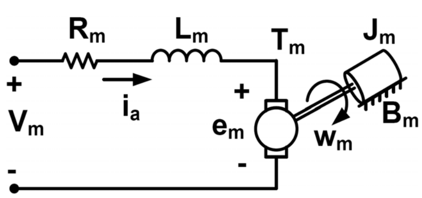

Fig. 3. The equivalent circuit of a dc motor.

A differential equation for the equivalent circuit can be derived by using Kirchhoff's voltage law around the electrical loop.

$$V_m(k) = R_m \, I_a(k) + L_m \frac{d\, I_a(k)}{dt} + E_m(k) \tag{1}$$

Where:

1. $E_m(k) = K_E \omega_m(k)$
2. i_1=constant; therefore $K_E = K_T$

The sum of torques of the motor must be equal zero, therefore,

$$T_e(k) - J\frac{d\omega_m(k)}{dt} - B\omega_m(k) - T_L(k) = 0 \tag{2}$$

The electromagnetic torque is proportional to the current through the armature winding and can be written as

$$T_e = K_T i_a \tag{3}$$

The load torque is given by

$$T_L = K_0 + K_1\omega_m + K_2\omega_m^2 \tag{4}$$

The nonlinear J and B have the following forms:

$$B_m = B_0 + B_1\omega_m + B_2\omega_m^2 \tag{5}$$

$$J_m = J_0 + J_1\omega_m + J_2\omega_m^2 \tag{6}$$

Where, the coefficients K_0, K_1, K_2, B_0, B_1, B_2, J_0, J_1 and J_2 are chosen as given in Appendix. The differential equations into state space form for the armature current and angular velocity can be written as

$$\frac{d}{dt}\begin{bmatrix} i_a \\ \omega_m \end{bmatrix} = \begin{bmatrix} -\frac{R_m}{L_m} & -\frac{K_t}{L_m} \\ \frac{K_t}{J} & -\frac{B}{J} \end{bmatrix}\begin{bmatrix} i_a \\ \omega_m \end{bmatrix} + \begin{bmatrix} \frac{1}{L_m} & 0 \\ 0 & -\frac{1}{J} \end{bmatrix}\begin{bmatrix} V_m \\ T_l \end{bmatrix} \tag{7}$$

Matlab/Simulink uses the Laplace Transform equations to simulate the motor dynamic operation. After taking the Laplace transform of each equation, they can be put into block diagram form. The block diagram for PMDC motor is shown in Fig. 4.

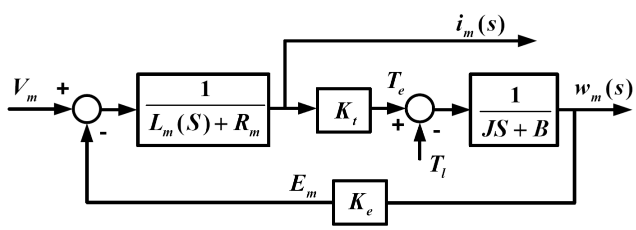

Fig. 4. Block diagram of PMDC motor.

The Simulink model for the PMDC motor is shown in below Fig. 5.

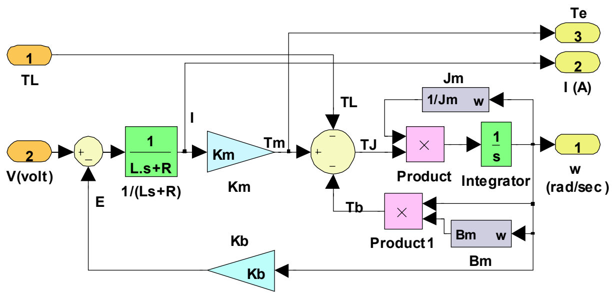

Fig. 5. The Matlab/Simulink functional model of the PMDC motor.

B. Photovoltaic Array

Photovoltaic system working principle is a converting solar energy into electrical energy directly. There are two most common used models of PV cell, one diode equivalent five parameters and four parameters circuit models. The first one is more complicated than the second one [23]. In this application, four parameters, which are functions of solar irradiance, load current and temperature, circuit model is realized. The arranged equivalent circuit model is shown in Fig. 6 [24], [25].

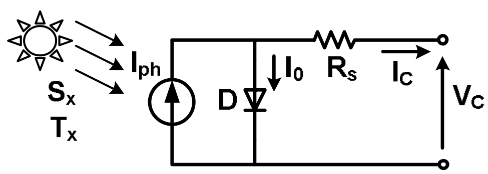

Fig. 6. One diode equivalent four parameters PV model.

The PV array equivalent circuit was modeled as a single block called PVA Model. This model simulates the characteristic of the solar panel with the equation given in Appendix.

III. PID TRI LOOP LIMITED CURRENT LOOP CONTROLLER WITH MOTOR CURRENT

PID stands for Proportional, Integral, Derivative. Controllers are designed to eliminate the need for continuous operator attention and used automatically adjust some variable to hold the process variable at the reference value. PID control scheme is shown in Fig. 7 [24], [25]. PID control system comprises three loops. The novel dynamic controller developed by the First Author comprises three supplementary regulating-loops, namely motor speed, current-limiter loop and minimum motor power loops. The dynamic power error $e_p(k)$ is defined

$$e_P = [P(k) - P(k-1)] / P_{base} \tag{8}$$

Where, $P=(V_m I_m)/(1+sT_2)$ is the average instantaneous motor power at a given instant. The global control error signal (e_t) is the sum of these three weighted supplementary loop errors, namely the motor speed, motor current and motor power multiplied by the three loop weighting factors (γ_w, γ_I and γ_P):

$$e_t = \gamma_w \cdot e_w + \gamma_I \cdot e_I + \gamma_P \cdot e_P \tag{9}$$

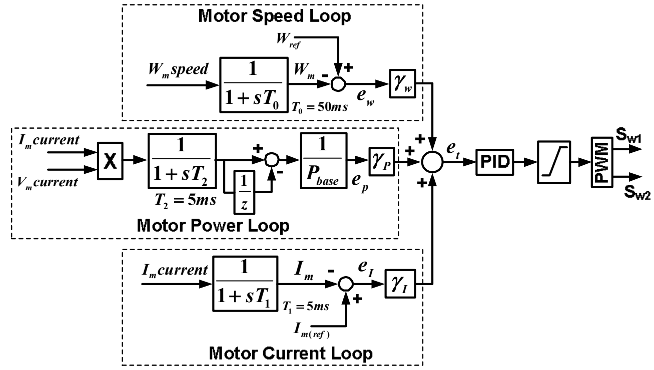

Fig. 7. Novel PID tri loop dynamic Controller with, speed, Current limiter and Minimum Source power loops.

The loop weighting factors (γ_w, γ_I and γ_P) are assigned for satisfactory fast and stable dynamic operation. The global error goes into PID controller block. After the signal is processed in the block, the PID controller output is limited by the limiter. The limited signal goes into PWM block and the block generates two pulses by comparing a triangular carrier waveform to a reference modulating signal. Two pulses are fed to the two-quadrant DC-DC chopper. The PMDC motor armature voltage is controlled by adjusting the switching functions for the chopper switches. Switch SW1 for the main speed regulation loop, while switch SW2 is used for the optional supplementary current limiting/braking loop [26].

IV. DIGITAL SIMULATION RESULTS

The simulation was run two times for each specified reference trajectory. The first one was to exhibit the system behavior at the constant speed reference. The second one was to demonstrate the controller performance for the variable speed reference trajectory. Figs. 8-15 depict the dynamic performance of the system with the speed reference set at 156 rad/s. Figs. 16-25 display the system outputs for the ramp up/step/ramp down speed reference trajectory. The proposed system scheme was digitally simulated by using the MATLAB/Simulink/Sim-Power Software and is shown in Fig. 26.

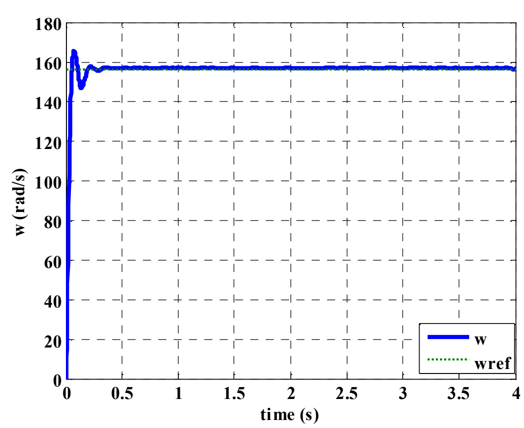

Fig. 8. Speed versus Time (wref=156rad/s).

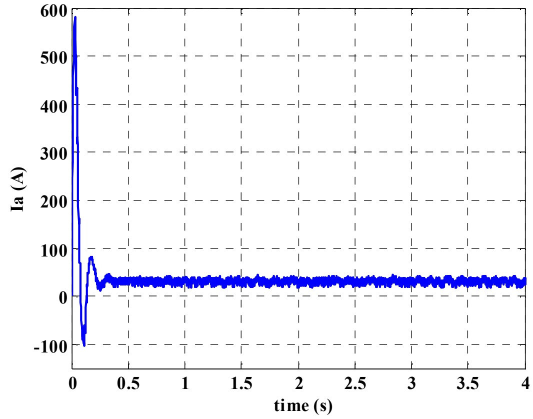

Fig. 9. Current (Ia) versus Time (wref=156rad/s).

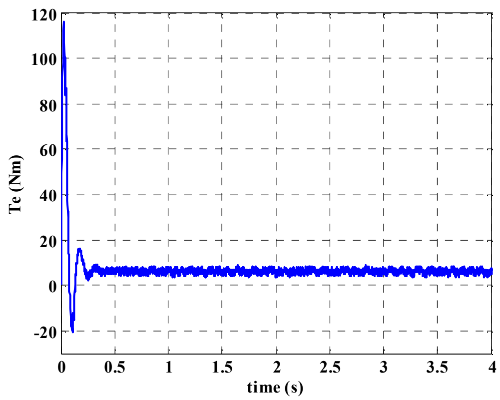

Fig. 10. Torque (Nm) versus Time (wref=156rad/s).

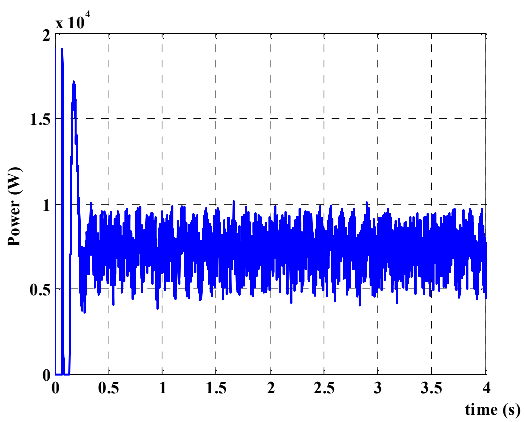

Fig. 11. Power (P) versus Time (wref=156rad/s).

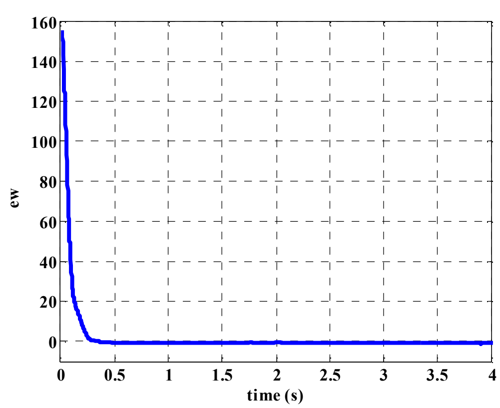

Fig. 12. Speed error (ew) versus Time (wref=156rad/s).

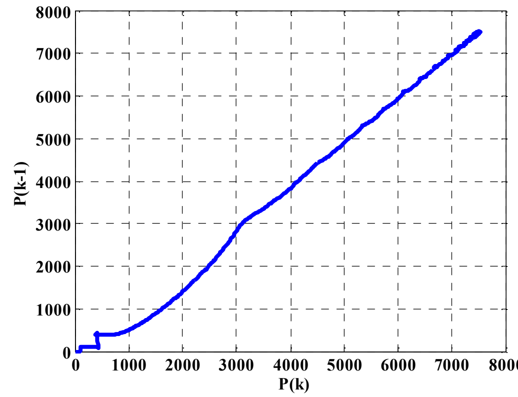

Fig. 13. P(k-1) versus P(k) (wref=156rad/s).

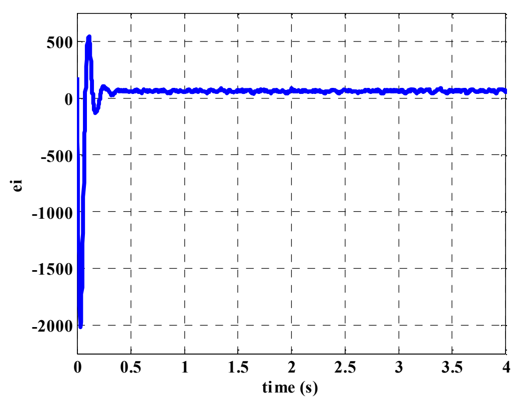

Fig. 14. Current error (e_I) versus Time (wref=156rad/s).

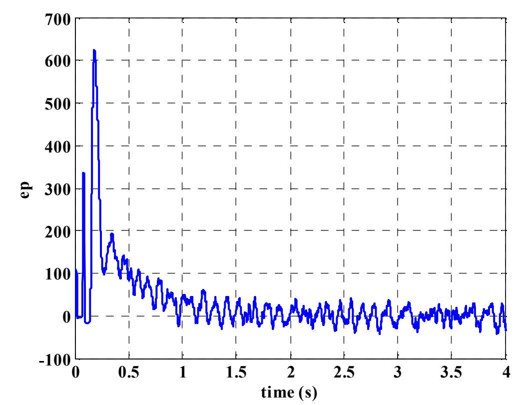

Fig. 15. Power error (e_P) versus Time (wref=156rad/s).

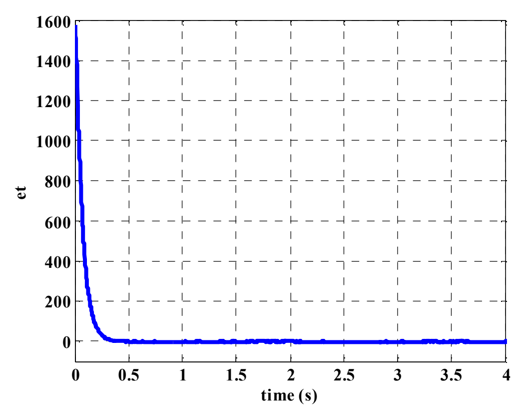

Fig. 16. Global error (et) versus Time (wref=156rad/s).

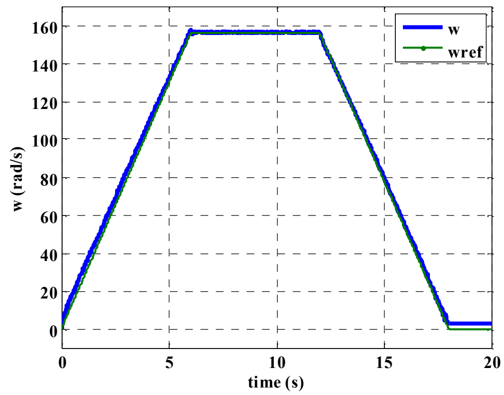

Fig. 17. Speed versus Time (wref=variable).

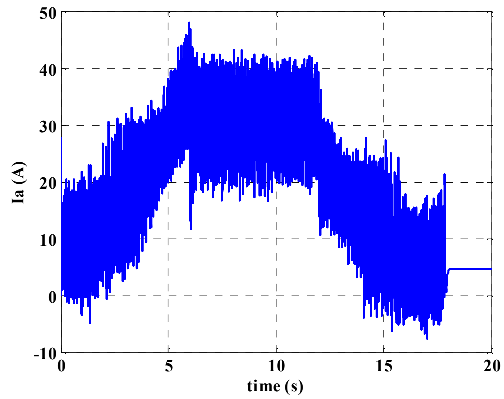

Fig. 18. Current (Im) versus Time (wref=variable).

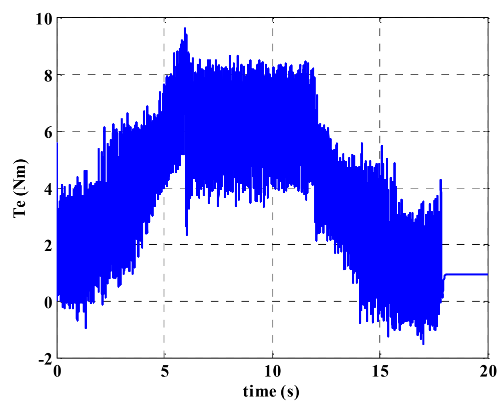

Fig. 19. Torque (Nm) versus Time (wref=variable).

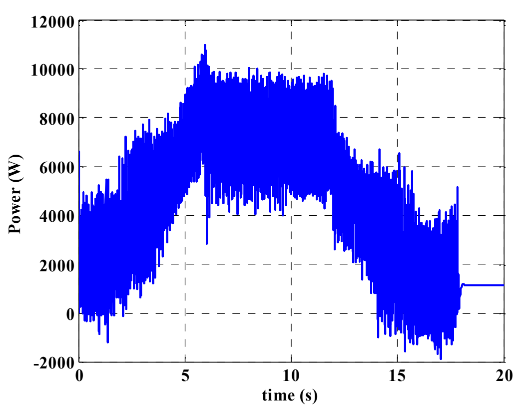

Fig. 20. Power (P) versus Time (wref=variable).

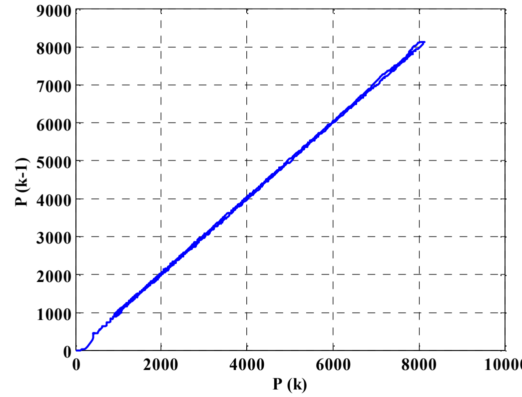

Fig. 21. P(k-1) versus P(k) (wref=variable).

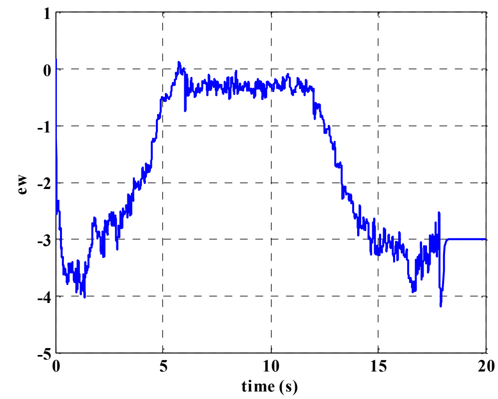

Fig. 22. Speed error (ew) versus Time (wref=variable).

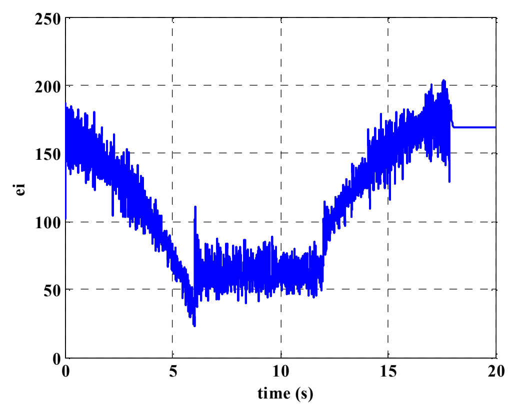

Fig. 23. Current error (e_I) versus Time (wref=variable).

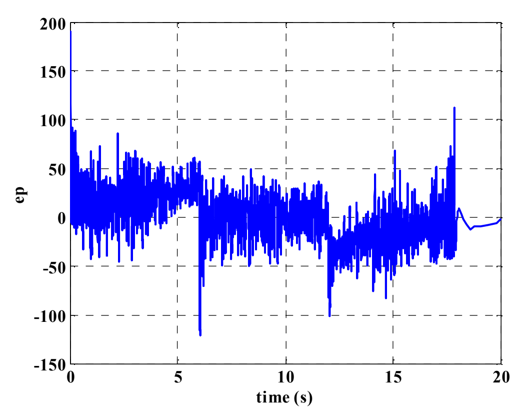

Fig. 24. Power error (e_P) versus Time (wref=variable).

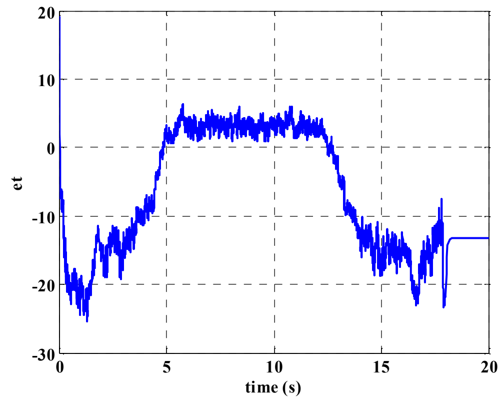

Fig. 25. Global error (et) versus Time (wref=variable).

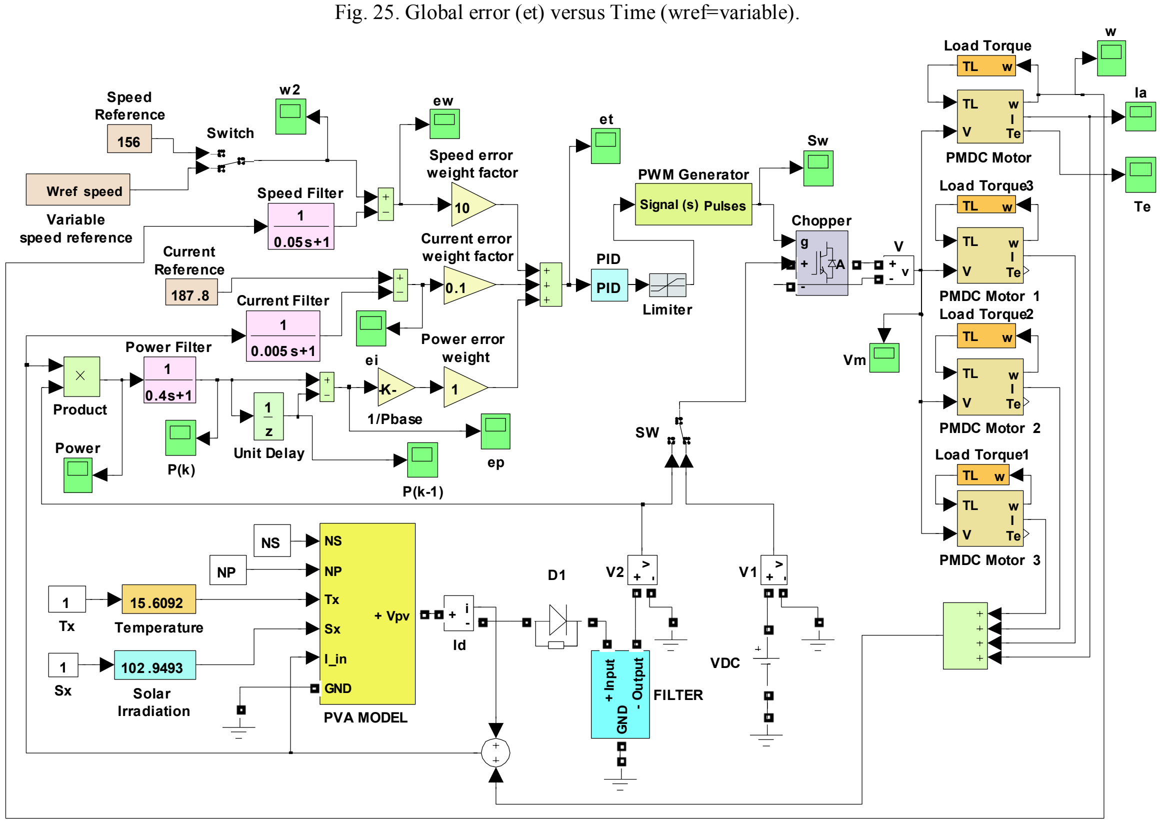

Fig. 26. The propose system scheme.

V. CONCLUSION

The paper presents a novel EV-Drive Scheme using a dual Photovoltaic and Battery electric source and independent Wheel Drive system. A tri loop dynamic PID controller with speed, current-limiter and minimum power utilization loops.. The dynamic performance of the control system is validated to be robust and accurate.

VI. APPENDIX

PV Array modeling equations:

$$V_{pv} = V_c * C_{TV} * C_{TI} * N_s$$

$$V_c = \frac{AKT_c}{e}\left(\frac{I_{ph} + I_0 - I_c}{I_0}\right) - R_s I_c$$

$$I_c = I_{pv} / N_p \text{ , } I_{pv} = C_{TI} * C_{SI} * I_{sc}$$

$$C_{TV} = 1 + \beta_T (T_c - T_x) \text{ , } C_{SV} = 1 + \beta_T \alpha_S (S_x - S_c)$$

$$C_{SI} = 1 + \frac{1}{S_c}(S_x - S_c) \quad C_{TI} = 1 + \frac{\gamma_T}{S_c}(T_x - T_c)$$

Where,
V_{pv}: Photovoltaic array output voltage (V)
V_c: Cell output voltage (V)
C_{TV}: Temperature-voltage coefficient
C_{SV}: Irradiation-voltage coefficient
N_s: Number of solar cells connected in series
A: Diode quality factor (6.2)
K: Boltzman' constant ($1.38*10^{-23}$J/K)
T_c: Photovoltaic cell operating temperature (K)

I_{ph}: Photocurrent, function of irradiation level and junction temperature (A)
I_0: Reverse saturation current of the diode D (0.01 A)
I_c: Cell output currrent (A)
e: Charge on an electron ($1.60*10^{-19}$ C)
R_s: Series resistance of the photovoltaic cell (0.002 Ω)
I_{pv}: Photovoltaic array current (A)
N_p: Number of solar cells connected in parallel
C_{SI}: Irradiation-current coefficient
C_{TI}: Temperature-current coefficient
I_{sc}: Cell short circuit currrent (A)
β_T : Temperature coefficient 1 (1/K)
T_x: Ambient temperature (K)
γ_T : Temperature coefficient 2 (1/K)
α_S : Irradiation coefficient
S_x: Ambient irradiation (%)
S_c: Photovoltaic cell operating irradiation (%)

Voltage source	V_m	36V
Inductance	L_m	3mH
Resistance	R_m	0.15 Ω
Induced voltage	e_m	V
Actual rated speed	$w_{a\text{-}rated}$	156 rad/s
Back emf constant	K_e	0.2 V.s/rad
Electromagnetic torque	T_e	Nm
Motor speed weighting factor	γ_w	10
Motor current weighting factor	γ_I	0.1
Motor power weighting factor	γ_P	1
Proportional constant	K_p	150
Integral constant	K_i	5
Derivative constant	K_d	2
Input filters R_f=0.05 Ω , L_f=0.05H, $C_f=20*10^{-6}$F		
Load torque constants K_0=0.9, $K_1=3.9*10^{-3}$, $K_2=66*10^{-6}$		
Viscous friction constants $B_0=5.7*10^{-3}$, $B_1=25*10^{-6}$, $B_2=0.423*10^{-6}$		
Rotor moment of inertia constants $J_0=14.44*10^{-3}$, $J_1=62.6*10^{-6}$, $J_2=1.06*10^{-6}$		

VII. ACKNOWLEDGMENT

I. H. Altas thanks the Scientific and Technological Research Council of Turkey (TUBITAK) for the financial support during this work.

REFERENCES

[1] E. Ozkop, “Sensorless BLDC control of permanent magnet axial flux motor”, MSc dissertation, Gent University, Belgium, July 2006.
[2] International Energy Outlook 2007*, Energy Information Administration (EIA), http://www.eia.doe.gov/iea.*
[3] K. Adachi, K. Ito and T. Fujishiro, “Study on a new four-wheel-steering control method at low speeds-front-end path memorizing method,” *Eighth International Conference on Automotive Electronics*, pp. 214-218, 1991.
[4] F. G. Pavuza, G. Beszedics, W. Toriser, M. Wawra and W. Winkler, “An improved electronic drive for small two and four wheel vehicles,” *IEEE Proceedings of the 1994, Southeastcon '94*, pp. 109-111, 1994.
[5] U. Chông, E. Namgoong, S. K. Sul, “Torque Steering Control of 4-Wheel Drive Electric Vehicle,” *IEEE Power Electronics in Transportation*, pp. 159-164, 1996.
[6] Y. Mori, E. Nakano, T. Takahashi and K. Takayama, “A study on the mechanism and control of omni-directional vehicle,” *IEEE/RSJ Proceedings of the International Conference, Intelligent Robots and Systems '96, IROS 96*, pp. 52-59, 1996.
[7] M. Terashima, T. Ashikage, T. Mizuno, K. Natori, N. Fujiwara and M. Yada, “Novel motors and controllers for high-performance electric vehicle with four in-wheel motors,” *IEEE Transactions on Industrial Electronics*, vol. 44, no. 1, pp. 28-38, 1997.
[8] S. Sakai, H. Sado and Y. Hori, “Motion control in an electric vehicle with four independently driven in-wheel motors,” *IEEE/ASME Transactions on Mechatronics,* vol. 4, no. 1, pp. 9-16, 1999.
[9] R. Pusca, Y. Ait-Amirat, A. Berthon and J.-M. Kauffmann, “Fuzzy-logic-based control applied to a hybrid electric vehicle with four separate wheel drives,” *IEE Proceedings Control Theory and Applications*, vol. 151, no. 1, pp. 73-81, 2004.
[10] Y. Hori, “Future vehicle driven by electricity and control-research on four-wheel-motored,“UOT Electric March II,” *IEEE Transactions on Industrial Electronics,* vol. 51, no. 5, pp. 954-962, 2004.
[11] R. Pusca, Y. Ait Amirat and A. Berthon, “Fuzzy logic speed estimator to drive a four electric wheels truck,” *The 4th Power Electronics and Motion Control Conference Proceedings, IPEMC 2004,* pp. 1448-1453, 2004.
[12] D. Kim, S. Hwang and H. Kim, “Rear motor control for a 4wd hybrid electric vehicle stability*,” IEEE International Conference on Vehicular Electronics and Safety*, pp. 86-91, 2005
[13] Z. Z. Liu, F. L. Luo, M. H. Rashid, “Speed nonlinear control of DC motor drive with field weakening,” *IEEE Transactions on Industry Applications*, vol. 39, no. 2, pp. 417-423, 2003.
[14] J. B. Lee, J. H. Choi, J. K. Chung, J. H. Lim, “Design and implementation of integrated drive circuit for a small BLDC motor,” Sixth *International Conference on Electrical Machines and Systems*, Nov. 9-11, 2003, vol. 2, pp. 491-494, 2003.
[15] A. M. Sharaf, C. Johnson, “A novel adaptive rule based speed controller for PMDC motor drives,” *IEEE International Symposium on Industrial Electronics, ISIE '95,* pp. 272-278, 1995.
[16] S. Saneifard, N. R. Prasad, H. A. Smolleck, J. J. Wakileh, “Fuzzy-logic-based speed control of a shunt DC Motor,” *IEEE Transactions on Education*, vol. 41, no. 2, pp. 159-164, 1998.
[17] S. Mehta, J. Chiasson, “Nonlinear control of a series DC motor: theory and experiment,” *IEEE Transactions on Industrial Electronics*, vol. 45, no. 1, pp. 134-141, 1998.
[18] A. A. El-Samahy, “Speed control of DC motor using adaptive variable structure control,” *IEEE 31st Annual Power Electronics Specialists Conference, PESC,* pp. 1118-1123, 2000.
[19] J. Y. M. Cheung, K. W. E. Cheng, A. S. Kamal, “Motor speed control by using a fuzzy logic model reference adaptive controller,” *IEE Power Electronics and Variable Speed Drives Conference,* pp. 430-435, 1996.
[20] S. Weerasooriya, M. A. El-Sharkawi, “Identification and control of a dc motor using back-propagation neural networks,” *IEEE Transactions on Energy Conversion,* vol. 6, no. 4, pp. 663-669, 1991.
[21] N. Barakat, R. Rajagopalan, “Speed control of a DC motor using a feedforward computed torque control scheme,” *IEEE International Symposium on Intelligent Control,* pp. 432-437, 1996.
[22] A. M. Sharaf, L. Yang, “An efficient photovoltaic dc village electricity scheme using a sliding mode controller,” *Proc. of the 2005 IEEE Conference on Control Applications,* August 28-31, 2005.
[23] A. A. Ghoneim, “Design optimization of photovoltaic powered water pumping systems,” *Energy Conversion & Management,* pp.1449-1463, 2006.
[24] I. H. Altas, A. M. Sharaf, “A novel GUI modeled fuzzy logic controller for a solar powered energy utilization scheme,” *Accepted for presentation at the 13th International Conference on Emerging Nuclear Energy Systems (ICENES2007), June 3-8, 2007, Istanbul, Turkey.*
[25] I. H. Altas**,** A. M. Sharaf, “A photovoltaic array simulation model for Matlab-Simulink GUI environment,” *Accepted for presentation at the International Conference on Clean Electrical Power, ICCEP’07, May 21-23, 2007, Capri, Italy.*
[26] A. I. Maswood, A. M. Sharaf, “A spice based fuzzy logic speed controller for PMDC motor drives,” *IEEE Intelligent Vehicles '94 Symposium*, pp. 423-428, 1994.